Sensors and Actuators B 209 (2015) 180–185

Contents lists available at ScienceDirect

Sensors and Actuators B: Chemical

journal homepage: www.elsevier.com/locate/snb

Acetone sensing of Au and Pd-decorated WO_3 nanorod sensors

Soohyun Kim, Sunghoon Park, Suyoung Park, Chongmu Lee*

Department of Materials Science and Engineering, Inha University, 253 Yonghyun-dong, Nam-gu, Incheon 402-751, Republic of Korea

ARTICLE INFO

Article history:
Received 14 August 2014
Received in revised form
17 November 2014
Accepted 18 November 2014
Available online 27 November 2014

Keywords:
Gas sensors
WO_3
Decoration
Acetone

ABSTRACT

The sensing properties of WO_3 nanorods decorated with both Pd and Au nanoparticles toward acetone were examined. AuPd-decorated WO_3 nanorods were prepared by immersing the WO_3 nanorods in an acetone/(25 mM) $HAuCl_4$/(25 mM) $PdCl_2$ solution followed by UV irradiation and annealing. The WO_3 nanorods decorated with Au and Pd nanoparticles exhibited a far stronger response to acetone gas that increased with increasing acetone concentration than the monometal-decorated counterparts. XPS analysis showed that considerable alloy formation has occurred during the annealing process of the Au and Pd nanoparticle-decorated WO_3 nanorods. Overall, Au and Pd particle-decoration had a synergistic effect on enhancing the sensitivity of the WO_3 nanorod sensor to acetone gas. The underlying mechanism of the enhanced response of the Au/Pd bimetallic particle-decorated WO_3 nanorods is also discussed.

1. Introduction

Semiconducting metal-oxides have many merits, such as simple fabrication methods, low cost and high compatibility with other processes [1–6], but their sensing performance at room temperature is unsatisfactory. Further improvements in their sensing performance are still a challenge. In many gas sensors, the electrical response is determined by the efficiency of the catalytic reactions of the gas-sensing material with the target gas. Therefore, techniques, such as decoration or doping with metal catalysts, are commonly used to enhance the catalytic activity of gas sensor materials.

Bimetallic catalyst nanoparticles, which are composed of two catalyst metal elements, often exhibit enhanced catalytic, electrocatalytic, electronic, magnetic, and optical properties compared to their parent metals due to synergistic effects. Over the past decade, a range of bimetallic catalysts have been studied including Pt-Pd, Pt-Au, Pt-Ni, Pt-Rh, Pt-Cu, Pt-Ag, Pd-Au, Pd-Cu, and Au-Ag bimetallic catalysts [7–10]. Of these bimetallic catalysts, Au-Pd bimetallic catalysts might have been used most widely because of their excellent catalytic activities for a range of reactions, such as CO oxidation, gas-phase hydrodehalogenation of fluorinated compounds, hydrogenation of 4-pentenoic acid, direct oxidation of hydrogen to form hydrogen peroxide, n-heptane isomerization, hydrodesulfurization of thiophenes, acetoxylation of ethene to vinyl acetate [11], and ethanol oxidation in alkaline media [12,13]. A variety of techniques have been employed to synthesize Pd/Au bimetallic nanoparticles, such as coprecipitation, ultrasound irradiation, and sequential reduction [14,15]. Most of these techniques are quite complicated. The enhanced catalytic activity of Au-Pd bimetallic catalysts is not completely understood. In the literature, the origin of the enhanced catalytic activity of bimetallic catalysts was attributed to geometric effects, electronic effects, participation of Au-Pd active sites, or reduction of a palladium hydride phase [16].

This study shows the enhanced sensing properties of tungsten trioxide (WO_3) nanorod sensors decorated with both Pd and Au nanoparticles toward acetone gas. In this study, Pd/Au bimetallic nanoparticles were synthesized by immersing tungsten trioxide (WO_3) nanorods in an acetone/$HAuCl_4$/$PdCl_2$ solution followed by UV irradiation and annealing. Acetone (CH_3COCH_3) is a good breath marker for the non-invasive diagnosis of diabetes [17,18]. Metal-oxide semiconductor gas sensors offer advantages in the detection of acetone gas, such as higher sensitivity, smaller size, lower cost, simpler operation, and better reversibility [19–21] compared to the techniques commonly used for detecting acetone, such as gas chromatography and mass spectrometry [22,23].

2. Experimental

2.1. Synthesis of WO_3 nanorods

WO_3 nanorods were synthesized by the thermal evaporation of a mixture of WO_3 and graphite powders in a quartz tube furnace. A mixture of WO_3 and graphite powders was placed at the center of a small quartz tube with an inner diameter of 20 mm. The quartz tube was then placed at the heating zone of a vacuum tube furnace. Subsequently, the system was evacuated for 10 min. The

* Corresponding author. Tel.: +82 32 860 7536; fax: +82 32 862 5546.
E-mail address: cmlee@inha.ac.kr (C. Lee).

http://dx.doi.org/10.1016/j.snb.2014.11.106
0925-4005/

temperature of the furnace was then increased to 1050 °C at a heating rate of 10 °C/min. As soon as the temperature reached 1050 °C, the O_2 and N_2 gas mixture was introduced into the quartz tube at 5 standard cubic centimetres per minute (sccm) and 95 sccm, respectively. The evaporation process for the synthesis of WO_3 nanorods lasted for 1 h. The O_2 gas supply was then stopped and the furnace was cooled to room temperature. Three different types of decoration were then performed on the WO_3 nanorods. First, to prepare the WO_3 nanorods decorated with Pd nanoparticles, the WO_3 nanorods were immersed in an ethanol/(50 mM) $PdCl_2$ solution, exposed to a UV laser beam (λ = 254 nm, I = 1.2 mW/cm^2) for 30 min and then annealed at 600 °C for 1 h in a N_2 atmosphere (flow rate: 100 sccm, pressure: 1 Torr). In a similar manner, the Au-decorated WO_3 nanorods were prepared by immersing the WO_3 nanorods in an ethanol/(50 mM) $HAuCl_4$ solution followed by UV irradiation and annealing. Finally, WO_3 nanorods decorated with both Au and Pd nanoparticles were prepared by immersing the WO_3 nanorods in an acetone/(25 mM) $HAuCl_4$/(25 mM) $PdCl_2$ solution under UV irradiation for 30 min followed by annealing at 600 °C for 1 h in a N_2 atmosphere (flow rate: 100 sccm, pressure: 1 Torr).

2.2. Characterization

The collected nanorod samples were examined by scanning electron microscopy (SEM, Hitachi S-4200), transmission electron microscopy (TEM, Philips CM-200) and X-ray diffraction (XRD, Philips X'pert MRD diffractometer). The crystallographic structure was determined by glancing angle XRD using Cu-K_α radiation (0.15406 nm) at a scan rate of 4°/min, and a 0.5° glancing angle with a rotating detector. X-ray photoelectron spectra (XPS) were performed on the three different types of samples: Pd particle-decorated WO_3 nanorods, Au particle-decorated WO_3 nanorods and Pd and Au particle-decorated WO_3 nanorods to examine the degree of alloy formation after annealing at 600 °C for 1 h.

2.3. Sensing tests

The gas sensing properties of the four different multiple networked nanorod sensors prepared from four different types of WO_3 nanorod samples: pristine WO_3 nanorods and Pd-decorated WO_3 nanorods, Au-decorated WO_3 nanorods and Pd and Au-decorated decorated WO_3 nanorods were measured. Each nanorod sample was dispersed ultrasonically in a mixture of deionised water (5 ml) and isopropyl alcohol (5 ml). A slurry droplet containing the nanostructure sample (10 μl) was placed onto 200 nm thick SiO_2-coated Si (1 0 0) substrates equipped with a pair of interdigitated (IDE) Ni (~200 nm)/Au (~50 nm) electrodes with a gap of 20 μm. A flow-through technique was used to test the acetone gas sensing properties. All measurements were performed in a temperature-stabilized sealed chamber with a constant flow rate of 200 cm^3/min at 300 °C under 50% RH. The acetone concentration was controlled by mixing acetone gas with synthetic air at different ratios. Detailed procedures for sensor fabrication and the sensing test are presented elsewhere [24]. The sensor response to the target gas was defined as $R_a/R_g \times 100$ (%), where R_a and R_g are the electrical resistances in the sensors in air and the target gas, respectively.

3. Results and discussion

Fig. 1(a) and (b), respectively, shows one-dimensional (1D) pristine and Au and Pd nanoparticle-decorated WO_3 nanostructures with a rod-like morphology and lengths ranging from 2 to 4 μm. A comparison of Fig. 1(a) and (b) reveals that the Au and Pd nanoparticle-decorated WO_3 nanostructures have somewhat larger diameter than the pristine WO_3 nanostructures. The inset in Fig. 1(b) showed that a typical WO_3 nanorod with a

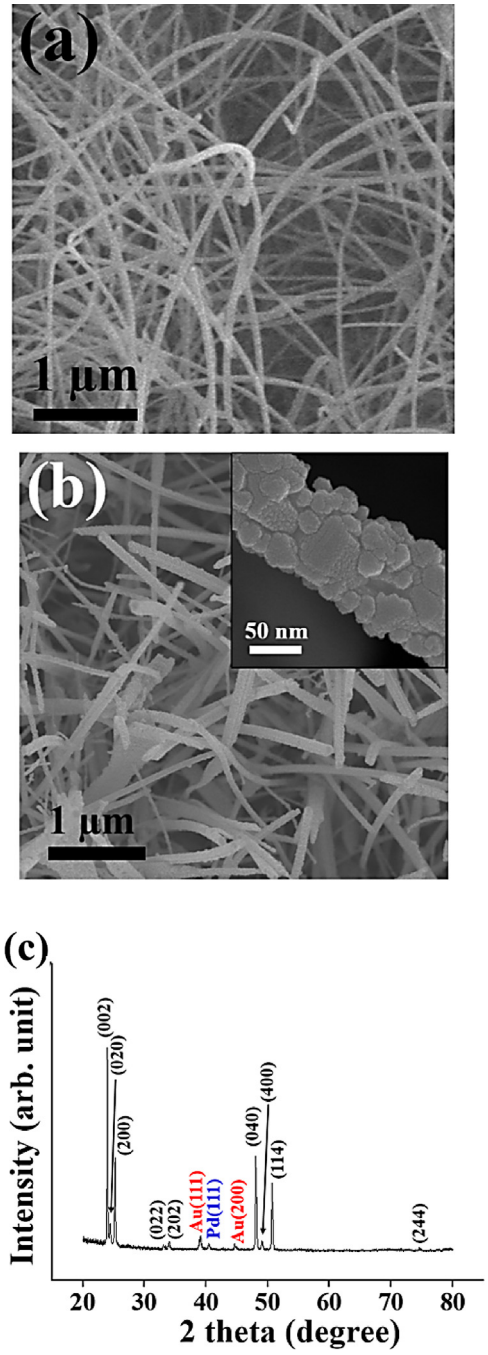

Fig. 1. (a) SEM image of pristine WO_3 nanorods, (b) SEM image of Au and Pd-decorated WO_3 nanorods, (c) XRD pattern of Au and Pd-decorated WO_3 nanorods.

diameter of ~100 nm were covered with many nanoparticles at various sizes. The XRD pattern of the Au and Pd-decorated WO_3 nanorods (Fig. 1(c)) showed two small reflection peaks assigned to face-centered cubic-structured Au with lattice constants of a = 0.4079 nm (JCPDS No. 89-3697), two small reflection peaks assigned to face-centered cubic-structured Pd with lattice constants of a = 0.390 nm (JCPDS No. 88-2335) as well as seven main peaks assigned to body-centered tetragonal-structured WO_3 with lattice constants of a = 2.044 nm and c = 0.3832 nm (JCPDS No. 72-1484). The existence of Pd and Au reflection peaks confirmed that the nanoparticles on the nanowires were crystalline and were composed of Au or Pd. The relatively weak reflection intensities of Au